Review Article

The Engine of Life Driven by Light – Structure of Photosystem II and the Mechanism of Water-splitting

Oxygenic photosynthesis is a process by which cyanobacteria, various algae and higher plants utilize light energy from the sun to split water and to convert carbon dioxide into carbohydrates using the reducing equivalents derived from water-splitting. Two products generated from this process are molecular oxygen and sugar; the former is the source of oxygen in the atmosphere and indispensable for aerobic life on the earth, whereas the latter provides the energy sustaining almost all life forms on the earth. Thus, photosynthesis is an important process for sustaining life activities on the earth.

The first reaction in photosynthesis is light-induced water-oxidation as depicted below:

$$2H_2O \xrightarrow{\text{Light}} 4e^- + 4H^+ + O_2$$

This reaction is catalyzed by an oxygen-evolving center (OEC) in photosystem II (PSII), a huge membrane-protein complex consisting of 17 trans-membrane subunits and 3 peripheral, hydrophilic subunits with a total molecular mass of 350 kDa for a monomer. PSII functions as a dimer located in the thylakoid membranes of oxygenic organisms, so its total molecular mass is 700 kDa.

The water-splitting reaction proceeds through the so-called S-state cycle [1,2], in which the catalyst adopts 5 different states denoted as S_i (where i= 0–4) (Fig. 1). The S_1-state is dark-stable; upon absorption of one photon, it advances to S_2 and subsequently to S_3, S_0 upon further absorption of photons. These transitions are accompanied by the release of electrons and protons. The S_4-state is a transient one, and molecular oxygen is formed and released during the transition from S_4 to S_0.

In order to unravel the mechanism of water-oxidation by PSII, it is essential to solve the crystal structure of PSII and its reaction intermediates. We purified the PSII dimer from a thermophilic cyanobacterium *Thermosynechococcus (T.) vulcanus*, and succeeded in its crystallization [3]. By optimizing the purification and crystallization conditions, we obtained high-quality crystals of PSII and solved its crystal structure at 1.9 Å using the synchrotron radiation (SR) X-rays at SPring-8 beamlines BL41XU and BL44XU [4]. This structure provided the first detailed picture of OEC, which is a Mn_4CaO_5-cluster organized in a distorted chair form. However, due to the strong, continuous synchrotron X-rays used, the structure has been suggested to suffer partially from X-ray radiation damage, which may cause partial reduction of the Mn ions and thus slightly longer distances in some of the Mn-Mn distances within the cluster. In order to obtain the radiation-damage free structure of OEC, we used the femtosecond X-ray free electron lasers (XFEL) provided by SACLA and a "fixed-target serial femtosecond crystallography" approach with large PSII crystals, and analyzed its structure at 1.95 Å resolution [5]. Furthermore, we employed a pump-probe approach in which, 2 laser flashes were used to "pump" the OEC to the S_3-state, and the serial femtosecond crystallography (SFX) method using PSII micro-crystals was used as the "probe" to detect structural changes occurred during the S-state transition from S_1-to-S_3 [6]. The results obtained from these studies allowed us to propose the mechanism for photosynthetic water-oxidation catalyzed by the Mn_4CaO_5-cluster.

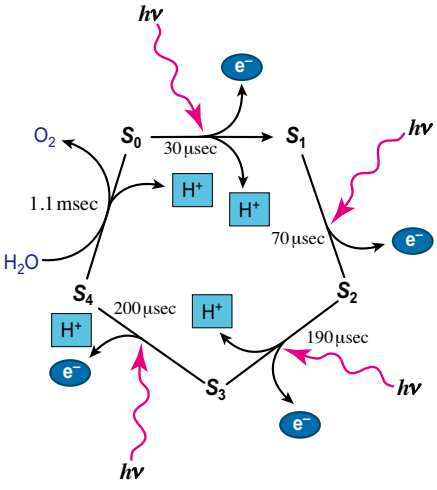

Fig. 1. S-state transition of the water-splitting reaction catalyzed by PSII.

The overall structure of PSII and the OEC

The overall structure of PSII analyzed at 1.9 Å resolution is depicted in Fig. 2(a). In this structure, 40 protein subunits were assigned, together with more than 150 cofactors. In addition, around 2,800 water molecules are found, which are mostly distributed in the two

membrane surfaces at the stromal and lumenal sides, demonstrating the typical feature of PSII as a membrane protein complex. The catalytic center for water oxidation was found to be a Mn_4CaO_5-cluster located at the lumenal surface. The Mn_4CaO_5-cluster is organized in a distorted chair form, with 3 Mn ions and 1 Ca ion connected by 4 oxygen atoms (oxo-bridges) forming the distorted chair base (cubane), and the 4th Mn connected to the outside of cubane (Fig. 2(b)). The metal ions are coordinated by 7 amino acid residues, among them, 6 are carboxyl ligands whereas 1 is a His ligand (Fig. 2(c)). Most of the carboxyl ligands are bidentate, and only 1 carboxyl ligand (D1-Glu189) and the His ligand are monodentate. In addition to the amino acid ligands, 4 water molecules were found to serve as terminal ligands; 2 of them are bonded to the Ca ion and 2 to the 4th Mn ion (Mn4). These ligands together make a saturated coordination environment for the metal ions; namely, all of the 4 Mn ions are 6-coordinated whereas the Ca ion is 7-coordinated. A number of additional water molecules were found around the cluster, suggesting that the metal cluster is located in a rather hydrophilic environment in the interior of the protein matrix. These water molecules are not coordinated directly to the metal ions but form extended hydrogen bonds (HBs) which are important for the release of protons [4,7].

The distortion found in the Mn_4CaO_5-cluster is caused by two main factors. One is the difference between the distances of Mn-O and Ca-O. The typical distances found between Mn-O are in the range of 1.8-2.1 Å, whereas that of Ca-O is in the range of 2.3-2.6 Å. The other factor is the differences between Mn-O. Among the 5 oxygen atoms found within the Mn_4CaO_5-cluster, O1-O4 have bond distances typical for manganese oxides (1.8-2.1 Å), whereas the O5 atom has unusually longer distance to its nearby Mn ions. Especially, the distance between O5-Mn1 and O5-Mn4 were found to be 2.6 Å and 2.5 Å, respectively. These results suggest that the binding of O5 to its nearby Mn ions are weak than the typical Mn-O bonds found for the other oxy-bridges, and thus the O5 atom may be cut out during the reaction cycle to provide one of the substrate oxygen for the O=O bond formation.

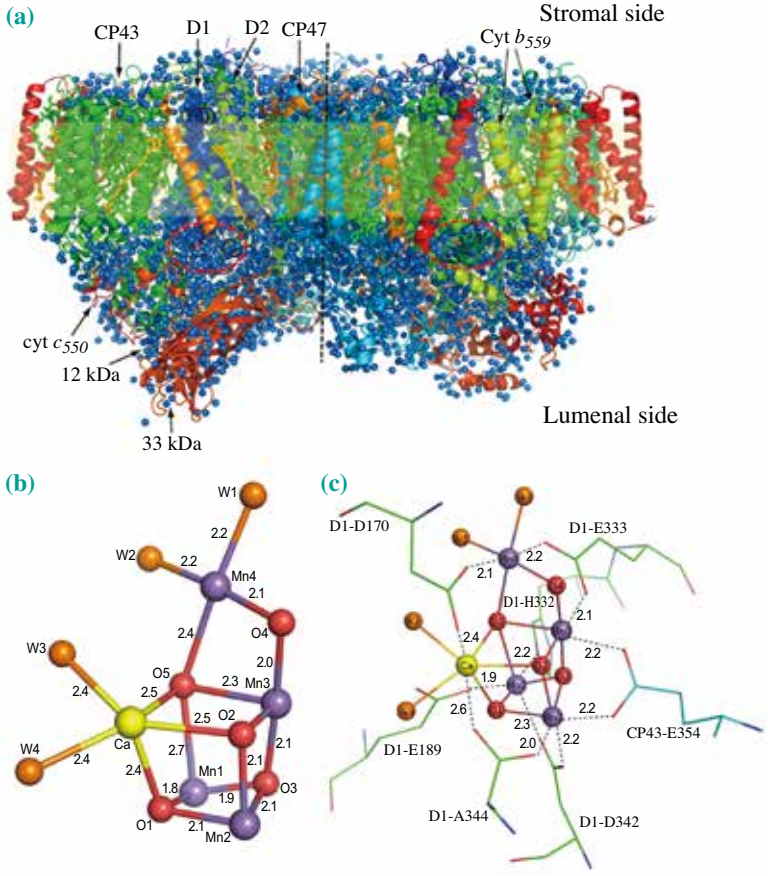

Fig. 2. Overall structure of the PSII dimer and that of OEC. **(a)** Overall structure of PSII dimer, with a view parallel to the membrane plane. The region painted in weak yellow represents the trans-membrane region, and blue balls represent water molecules. The areas circled by red dotted lines represent the site where OEC is located. **(b)** The structure of OEC, the Mn_4CaO_5-cluster. Numbers represent inter-atomic distances in Å. **(c)** Amino acid ligands of the Mn_4CaO_5-cluster.

The distorted shape of the Mn_4CaO_5-cluster suggests that it is rather instable, a distinct feature important for the catalytic activity. During the S-state cycle, the catalyst is believed to undergo subtle structural changes to advance to the higher S-states. This has been proven by various spectroscopic studies including X-ray absorption, electron paramagnetic resonance, infrared spectroscopy, etc. [8] The instable, or flexible nature of the Mn_4CaO_5-cluster implies that it can easily undergo structural changes to advance the catalyst to the intermediate states, enabling it to catalyze the water-splitting reaction efficiently.

The structural features discussed above were based on the structure solved using SR X-rays at SPring-8, and questions arose that it has suffered from some radiation damage, resulting in the reduction of some Mn ions and thus an elongation in some of the Mn-Mn pairs as well as the Mn-O distances. In fact, X-ray spectroscopic measurements [8] and theoretical calculations [9-11] based on the crystal structure we solved have suggested some slightly shorter Mn-Mn distances than that were observed in the crystal structure.

Radiation damage-free structure of the Mn_4CaO_5-cluster

In order to remove the possible radiation damage and obtain the structure of the Mn_4CaO_5-cluster in its native state, we employed the femtosecond XFEL from SACLA to collect the diffraction data. To solve the radiation damage-free structure of PSII at a sufficiently high resolution, we used large PSII crystals (1.0 mm × 0.4 mm × 0.15 mm) at a cryogenic temperature, and adopted a fixed-target serial femtosecond crystallography method [12]. This was done by illuminating one point of the crystal with a pulse of XFEL, and then move the crystal by 50 μm with a rotation of 0.2° to obtain a continuous, fresh diffraction image. By using more than 100 large PSII crystals, we were able to obtain one full diffraction data set. In order to ensure the reproducibility, we collected two independent data sets to obtain average inter-atomic distances. The results showed that most of the Mn-Mn distances are shorter by 0.1–0.3 Å compared with the structure obtained by SR X-rays (Fig. 3(a)). Some of the Mn-O and Mn-ligand distances also changed slightly. However, the feature of the unusually longer distances between O5 and its nearby Mn ions was retained, although the Mn1-O5, Mn4-O5 distances were changed to 2.7 Å, 2.3 Å respectively (Fig. 3(b)) [5]. This suggests that O5 may participate in the O=O bond formation, and its binding to Mn1 at the S_1-state is very weak.

Light-induced structural changes and the site of O=O bond formation

The structure solved above corresponds to the catalyst at the S_1-state before the water-splitting reaction starts. In order to unravel the mechanism of water-splitting and O=O bond formation, it is essential to solve the structures of the Mn_4CaO_5-cluster at the reaction intermediate states (S-states other than S_1). To this purpose, we employed a "pump-probe" approach in which, 2 laser-flashes separated by 10 msec were used to "pump" the Mn_4CaO_5-cluster to the S_3-state, which is a state immediately before the O_2 release, and XFEL pulses were used as the probe to detect the structural changes at room temperature [6]. To obtain a high efficiency of excitation by the 2 flashes, PSII micro-crystals were used, for which the SFX method is the most suitable approach to collect the X-ray diffraction data. The data obtained was used to calculate the Fourier difference map between the S_3 and S_1-states, which showed structural changes at both the electron donor and acceptor sides (Fig. 4).

At the electron acceptor side, the secondary electron acceptor Q_B was found to rotate slightly, along with some small changes in its vicinity (Fig. 4(a)). This causes a slight shortening of the H-bond between the head of Q_B and D1-

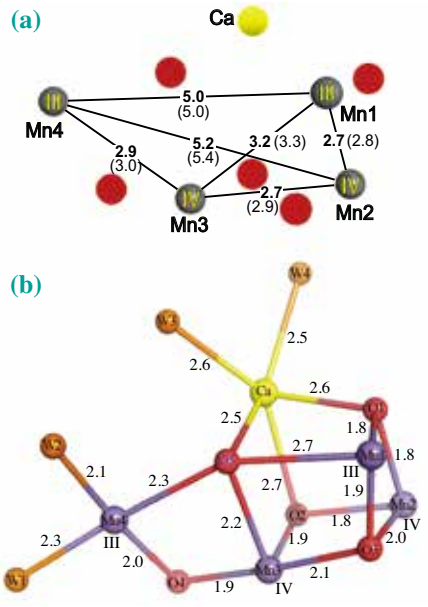

Fig. 3. Radiation damage-free structure of the Mn_4CaO_5-cluster. **(a)** Mn-Mn distances (numbers in parentheses are the distances determined by SR previously [4]). **(b)** Mn-O and Ca-O distances.

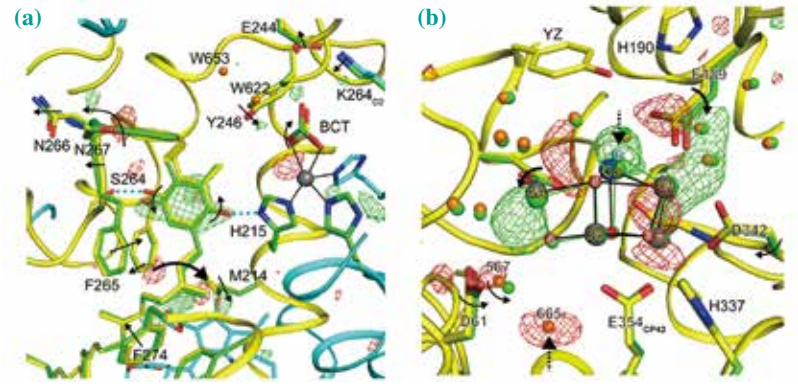

Fig. 4. Fourier difference electron density maps between the 2-flashes illuminated S_3-state and the S_1-state, and their corresponding structural changes. **(a)** The region of the acceptor (reducing) side. **(b)** The region of the donor (oxidizing) side. In both panels, green represents positive and red represents negative Fourier difference maps contoured at ±5.0 σ.

Ser264. This is explained to reflect that, upon 2-flashes illumination, a part of Q_B remains reduced due to the short time interval between the flash illumination and the XFEL pulses as well as the crystal environment that may limit the efficiency of electron transfer from Q_A to Q_B, which enhances the H-bond between Q_B and D1-Ser264, resulting in the shortening of their distance [6]. This in turn suggests that the 2 flashes illumination employed was successful in advancing the S-states.

At the donor (oxidizing) side, two major changes were found. One is the appearance of a strong negative density at the position of water-665 (W665), suggesting that this water molecule becomes mobile upon 2-flashes illumination (Fig. 4(b)) [6]. This water is H-bonded with O4 through another water molecule W567, and this H-bond was broken after 2-flashes illumination. This is considered to reflect a proton transfer occurring through the O4-W567-W665 H-bond network that extends to the bulk solution at the lumenal side, during the S_1-S_3 transition [7,13].

The second large change observed at the donor side is the appearance of a strong positive density at a position close to O5. This positive density could be modeled as a new water molecule (O6), which has a distance of 1.5 Å and coordinated to Mn1 directly [6]. This suggests that a new water molecule is inserted during the transition from S_1 to S_3 (mostly from S_2 to S_3), which is able to form the O=O bond with O5 (Fig. 5). Thus, the O5 atom provides one of the substrate oxygen atoms; upon its release in the following S-state transition, a new water molecule is expected to come in to occupy the vacant position and returns the catalyst to the S_0-state.

In conclusion, a combination of high-resolution structural analysis using SR of SPring-8 and time-resolved "pump-probe" structural analysis using XFEL of SACLA allowed us to solve the structure and reaction mechanism of the catalytic center for photosynthetic water oxidation, the Mn_4CaO_5-cluster, coordinated within the huge membrane protein complex PSII. These results provide important clues for the development of artificial catalysts for water-splitting using visible light, an important step toward acquisition of clean, renewable energy from the sun, which will greatly contribute to the realization of a sustainable society.

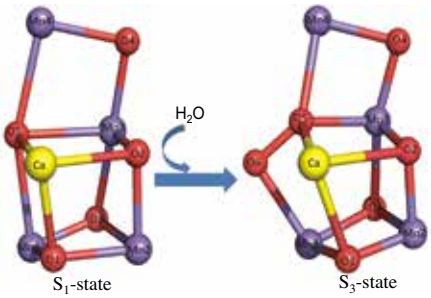

Fig. 5. Structural changes of the Mn_4CaO_5-cluster upon transition from the S_1-state to the S_3-state induced by 2-flashes illumination.

Jian-Ren Shen

Research Institute for Interdisciplinary Science, Okayama University

Email: shen@cc.okayama-u.ac.jp

References

[1] P. Joliot *et al.*: Photochem. Photobiol. **10** (1969) 309.
[2] B. Kok *et al.*: Photochem. Photobiol. **11** (1970) 457.
[3] J.-R. Shen, N. Kamiya: Biochemistry **39** (2000) 14739.
[4] Y. Umena *et al.*: Nature **473** (2011) 55.
[5] M. Suga *et al.*: Nature **517** (2015) 99.
[6] M. Suga *et al.*: Nature **543** (2017) 131.
[7] J.-R. Shen: Annu. Rev. Plant Biol. **66** (2015) 23.
[8] J. Yano and V. Yachandra: Chem. Rev. **114** (2014) 4175.
[9] K. Kanda *et al.*: Chem. Phys. Lett. **506** (2011) 98.
[10] S. Yamanaka *et al.*: Chem. Phys. Lett. **511** (2011) 138.
[11] M.R. Blomberg *et al.*: Chem. Rev. **114** (2014) 3601.
[12] K. Hirata *et al.*: Nat. Methods **11** (2014) 734.
[13] K. Saito *et al.*: Nat. Commun. **6** (2015) 8488.